Rational Synthesis of Unidimensional Mixed Valence Solids. Structure–Oxidation State–Charge Transport Relationships in Iodinated Nickel and Palladium Bisbenzoquinonedioximates

Leo D. Brown,[1a] Davida Webster Kalina,[1a] Malcolm S. McClure,[1b] Steven Schultz,[1c] Stanley L. Ruby,[1c] James A. Ibers,*[1a] Carl R. Kannewurf,*[1b] and Tobin J. Marks*[1a,2]

Contribution from the Department of Chemistry, the Department of Electrical Engineering, and the Materials Research Center, Northwestern University, Evanston, Illinois 60201, and the Physics Division, Argonne National Laboratory, Argonne, Illinois 60439. *Received August 23, 1978*

Abstract: This paper presents a detailed study of crystal structure, stoichiometry, oxidation state, and electron transport in the materials $Ni(bqd)_2$, $Pd(bqd)_2$, $Ni(bqd)_2I_{0.018}$, $Ni(bqd)_2I_{0.5}{\cdot}S$, and $Pd(bqd)_2I_{0.5}{\cdot}S$, where bqd = *o*-benzoquinonedioximato and S = an aromatic solvent. The compound $Pd(bqd)_2I_{0.50}{\cdot}0.52o\text{-}C_6H_4Cl_2$ has been shown by single-crystal X-ray diffraction to crystallize in the tetragonal space group $D_{4h}{}^2\text{-}P4/mcc$, with four formula units in a cell of dimensions $a = 16.048$ (7) and $c = 6.367$ (3) Å. Full-matrix least-squares refinement gave a final value of the conventional R index (on F) of 0.052 for 1278 reflections having $F_o{}^2 > 3\sigma(F_o{}^2)$. The crystal structure consists of stacked $Pd(bqd)_2$ units, each staggered by 65° with respect to its nearest neighbors, and disordered chains of iodine atoms extending in the c direction. The solvent molecules are disordered throughout tunnels which extend parallel to c. The Pd–Pd distance is 3.184 (3) Å, Pd–N = 1.996 (7) Å, and the $Pd(bqd)_2$ units are rigorously planar. Resonance Raman studies (ν_0 4880–6471 Å) of $Pd(bqd)_2I_{0.5}{\cdot}S$ and $Ni(bqd)_2I_{0.5}{\cdot}S$ indicate that the predominant form of the iodine present is $I_3{}^-$ ($\nu_{\text{fundamental}}$ 107 cm^{-1}), hence that the formal charge on the $M(bqd)_2$ units is +0.17 (2). Iodine-129 Mössbauer studies are also consistent with the $I_3{}^-$ formulation. Optical spectra of these complexes exhibit a strong, broad transition at 600 nm which is largely, if not exclusively, due to the polyiodide chains. Crystallization of $Ni(bqd)_2$ from benzene containing traces of iodine produces the new orthorhombic phase $Ni(bqd)_2I_{0.018}$. Single-crystal X-ray studies have shown it to crystallize in the space group $D_{2h}^{26}\text{-}Ibam$ with four formula units in a unit cell of dimensions $a = 16.438$ (2), $b = 14.759$ (4), and $c = 6.360$ (2) Å. Full-matrix least-squares refinement gave a final value of the conventional R index (on F) of 0.11 for 1026 reflections having $F_o{}^2 > 3\sigma(F_o{}^2)$. The structure contains rigorously planar $Ni(bqd)_2$ units stacked along the c axis with each molecule staggered by 68° with respect to its nearest neighbors. The Ni–Ni distance is 3.180 (2) Å and Ni–N = 1.88 (10) Å. Structural relationships are discussed for all $M(bqd)_2$ and $M(bqd)_2I_x$ compounds; partial oxidation results in a small contraction of the interplanar spacings of 0.019 Å (Pd) to 0.027 Å (Ni). Single-crystal electrical conductivity measurements (dc and 100-Hz ac) in the stacking direction show an increase in conductivity upon partial oxidation of $>10^3$ (Ni) and $>10^4$ (Pd). Maximum conductivities at 300 K are $Ni(bqd)_2I_{0.52}{\cdot}0.32C_6H_5CH_3 = 1.1 \times 10^{-5}$ $(\Omega\ cm)^{-1}$ and $Pd(bqd)_2I_{0.5}{\cdot}0.52o\text{-}C_6H_4Cl_2 = 8.1 \times 10^{-3}$ $(\Omega\ cm)^{-1}$. Variable-temperature studies show that the electrical conductivity follows, over the entire range investigated, an exponential temperature dependence with a single activation energy: 0.54 ± 0.08 (Ni) and 0.22 ± 0.03 eV (Pd).

In an accompanying article[3] we discuss the properties of stacked, partially oxidized bisdiphenylglyoximates of nickel and palladium, $M(dpg)_2I$, A. It was found that the iodine in these materials was present predominantly, if not exclusively, as $I_5{}^-$, hence that the $M(dpg)_2$ units possess formal frac-

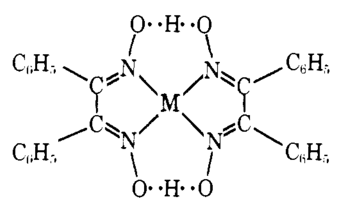

A

M = Ni, Pd

tional oxidation states representable approximately as $[M(dpg)_2]_5{}^+I_5{}^-$. Though the iodine oxidation produces a 10^7–10^8 increase in dc electrical conductivity, the facility of electron transport in these materials is still less than that of $K_2Pt(CN)_4Br_{0.3}{\cdot}3H_2O$[4] and several other classes of partially oxidized metallomacrocycles that we have recently synthesized.[5] It was thus of interest to explore the effect of chemical functionalization on the metal bisglyoximate core. A means to decrease stacking distances and to elaborate conjugation was evident in the planar nickel and palladium complexes of benzoquinonedioxime, $M(bqd)_2$, B.[6] The earlier work of Endres and co-workers[7,8] established the existence of quasi-one-dimensional materials of reported stoichiometry $M(bqd)_2I_{0.5}$, M = Ni, Pd. The nickel complex was reported to possess a tetragonal ($P4/mcc$) crystal structure with stacks of partially staggered $Ni(bqd)_2$ units (Ni–Ni = 3.153 (3) Å) and disor-

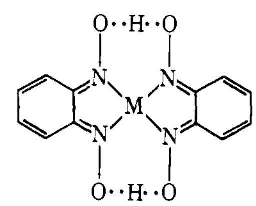

B

M = Ni, Pd

dered chains of iodine-containing species running parallel to the c direction.[8] It was proposed that iodine was present as $I_3{}^-$, though this conclusion could not be derived from the Bragg diffraction pattern. The crystal structure of the uniodinated precursor, $Ni(bqd)_2$, was found to be monoclinic ($P2_1/n$) by Leichert and Weiss[9] and to consist of canted bis(benzoquinonedioximato)nickel units. In contrast, the structure of $Pd(bqd)_2$ is orthorhombic ($Imcb$) with stacked $Pd(bqd)_2$ moieties extending along the c axis.[10]

Though the aforementioned work provided an important initial glimpse of the range of bisbenzoquinonedioximate structures and compositions obtainable, several important questions remained unanswered. First, the nature of the iodine in the $M(bqd)_2I_{0.5}$ species was undetermined. Thus, it was impossible to say with certainty whether the iodinated nickel

0002-7863/79/1501-2937$01.00/0

and palladium bisbenzoquinonedioximates were actually mixed valence (partially oxidized) materials or not. Second, the available structural data did not provide a clear picture as to what geometrical changes, if any (e.g., in the metal-metal stacking distances), accompanied iodination. The canted monoclinic $Ni(bqd)_2$ and stacked tetragonal $Ni(bqd)_2I_{0.5}$ structures could not be meaningfully compared in the sense that the stacked $Ni(dpg)_2$ and $Ni(dpg)_2I$ structures could.[3] In addition, structural data on $Pd(bqd)_2I_{0.5}$ were not available for comparison with the existing orthorhombic $Pd(bqd)_2$ structure. Finally, little was known about the charge transport properties of $M(bqd)_2I_{0.5}$ single crystals vis-à-vis those of $M(bqd)_2$.[11] In a preliminary communication[12] we reported a resonance Raman and iodine-129 Mössbauer study of $Ni(bqd)_2I_{0.5}$ which showed the iodine to be present predominantly as I_3^-, hence that the charge distribution could be represented by formal fractional oxidation states as depicted by $[Ni(bqd)_2]_6{}^+I_3^-$. Independent of this work, analysis[13] of the diffuse X-ray scattering pattern arising from the disordered iodine chain structure in $Ni(bqd)_2I_{0.5}$ reached exactly the same conclusion concerning the form of the iodine: I_3^-. In this paper we present a full exposition of our chemical, spectral, structural, and charge transport investigations within the nickel and palladium bisbenzoquinonedioximate series. This discussion includes a reformulation of the actual composition of the $M(bqd)_2I_{0.5}$ materials, the structural characterization of $Pd(bqd)_2I_{0.5}\cdot 0.52o\text{-}C_6H_4Cl_2$, the synthesis and structure elucidation of a new, orthorhombic $Ni(bqd)_2I_{0.018}$ compound, comments on $M(bqd)_2I_x$ optical spectra,[14] and a comparison of the geometrical, partial oxidation state, and charge transport characteristics in all of the aforementioned materials.

Experimental Section

All solvents and chemicals were reagent grade. Benzene, toluene, and hexane were freshly distilled from sodium-potassium alloy under nitrogen; *o*-dichlorobenzene was dried over Davison 4A molecular sieves. The ligand *o*-benzoquinonedioxime (bqdH) was synthesized by the reduction of *o*-dinitrosobenzene with sodium borohydride as described elsewhere.[15] Elemental analyses were by Ms. H. Beck, Northwestern Analytical Services Laboratory, Micro-Tech Laboratories, Galbraith Laboratories, or Alfred Bernhardt Microanalytical Laboratories. Analysis of Ni and I by neutron activation was performed by General Activation Analysis, Inc. Mass spectra were recorded on a Hewlett-Packard 5930 instrument by Dr. D. Hung. Iodinated materials were routinely stored at −20 °C in the dark.

Bis(benzoquinonedioximato)nickel(II), $Ni(bqd)_2$. This complex was prepared by the room temperature reaction of $NiCl_2\cdot 6H_2O$ with bqdH in ethanol-water. The reaction is complete within 0.5 h. The crude, dark-brown $Ni(bdq)_2$ was collected by suction filtration, washed with distilled water, washed with methanol, and then dried for several hours at 110 °C. The crude product was finally Soxhlet extracted (twice) with benzene to yield a dark-brown, microcrystalline solid. Yields of $Ni(bqd)_2$ from this procedure were typically about 80%. Large crystals (elongated platelets) for transport studies were grown by very slow cooling of hot toluene solutions.

Anal. Calcd for $C_{12}H_{10}N_4O_4Ni$: C, 43.28; H, 3.03; N, 16.83. Found: C, 43.21; H, 2.96; N, 16.74.

Infrared data (Nujol mull, cm^{-1}): 3090 w, 1600 s, 1500 s, 1265 s, 1140 m, 1080 s, 950 (br), 820 w, 740 vs, 610 m.

Bis(benzoquinonedioximato)palladium(II), $Pd(bqd)_2$. The procedure for the synthesis and purification of this compound was analogous to that described above for $Ni(bqd)_2$ except that the $PdCl_2$ starting material was solubilized by treatment with a small amount of hydrochloric acid. The final product, $Pd(bqd)_2$, is a dark-green, microcrystalline solid. Larger crystals can be grown by slow cooling of hot toluene solutions.

Anal. Calcd for $C_{12}H_{10}N_4O_4Pd$: C, 37.86; H, 2.65; N, 14.72. Found: C, 37.78; H, 2.60; N, 14.68.

Infrared data (Nujol mull, cm^{-1}): 1600 s, 1520 vw, 1490 s, 1415 s, 1355 s, 1285 vs, 1185 m, 1165 m, 1130 w, 1060 vs, 965 w, 880 m, 790 m, 740 s, 730 s, 615 m.

Bis(benzoquinonedioximato)palladium·0.50 iodine·0.52*o*-dichlorobenzene, $Pd(bqd)_2I_{0.5}\cdot 0.52o\text{-}C_6H_4Cl_2$. Solutions of $Pd(bqd)_2$ in *o*-dichlorobenzene (4.5×10^{-3}M) were heated to 90 °C and were then made 4.0×10^{-2} M in triply sublimed iodine. The resulting mixture was next filtered while hot, and the filtrate rewarmed to 90 °C. The hot solution was then allowed to cool to ambient temperature over a period of 3-5 days. At this time the cooled solution was suction filtered, and the solid product was washed repeatedly with cold hexane and then dried in air. Dark, needle-like crystals of the desired product possessed a golden luster and were typically 3-15 mm in length. These crystals were mechanically separated from the noncrystalline and microcrystalline material. The yield of golden crystals obtained in this manner was ca. 40%. On the basis of the elemental analysis of the bulk material, the stoichiometry $Pd(bqd)_2I_{0.5}\cdot 0.52o\text{-}C_6H_4Cl_2$ is assigned.

Anal. Calcd for $C_{15.12}H_{12.03}N_4O_4PdI_{0.5}Cl_{1.04}$: C, 34.91; H, 2.34; N, 10.78; I, 12.13; Cl, 7.06. Found: 34.56; H, 2.34; N, 10.82; I, 12.19; Cl, 7.09. Analyses (C,H,N, Bernhardt) on each of three single crystals weighing 0.372, 0.500, and 0.675 mg indicated an average incorporation of *o*-dichlorobenzene corresponding to $Pd(C_6H_5N_2O_2)_2I_{0.52(2)}(o\text{-}C_6H_4Cl_2)_{0.41(2)}$.

Mass spectra of the above crystals (10- or 70-eV ionizing voltage) recorded with source and probe temperatures of 200 and 100 °C, respectively, revealed the parent ions and fragmentation patterns characteristic of iodine and *o*-dichlorobenzene.[16a]

Infrared data (Nujol mull, cm^{-1}): 1600 s, 1520 vw, 1490 s, 1415 s, 1355 s, 1280 vs, 1185 m, 1160 m, 1130 w, 1065 vs, 970 w, 880 w, 790 w, 740 s, 730 s, 615 m.

When the above synthetic procedure was carried out with increased iodine concentrations (4.9, 5.9, 6.9, 7.9×10^{-2} M) the yield of golden crystals decreased and the appearance of a dark, shiny, rather flaky material was noted. For the above four experiments, the product analyzed as $Pd(bqd)_2I_x$, where x = 1.5-2.0. As an example, the product obtained when a solution of $Pd(bqd)_2$ (4.5×10^{-3} M) in hot *o*-dichlorobenzene was made 7.9×10^{-2} M in iodine analyzed as $Pd(bqd)_2I_{1.8}$.

Anal. Calcd for $C_{12}H_{10}N_4O_4PdI_{1.8}$: C, 23.66; H, 1.65; N, 9.20; I, 37.50. Found: C, 24.03; H, 1.05; N, 9.08; I, 36.72.

The infrared spectrum was identical with those of the other $Pd(bqd)_2I_x$ materials. The resonance Raman spectrum (ν_0 5145 Å) displayed prominent scattering at 107 m, 174 vs, 215 w, and 360 m cm^{-1}.

Bis(benzoquinonedioximato)nickel·0.52iodine·0.32toluene, $Ni(bqd)_2I_{0.52}\cdot 0.32C_7H_8$. Solutions of $Ni(bqd)_2$ (6.0×10^{-3} M) and triply sublimed iodine (4.0×10^{-2} to 4.4×10^{-2} M) in toluene at 90 °C were treated in a manner analogous to the previously described procedure involving $Pd(bqd)_2$ in *o*-dichlorobenzene. Large, needle-like crystals exhibiting a golden luster could be isolated from the toluene solutions in ca. 20% yield.

Anal. Calcd for $C_{14.24}H_{12.56}N_4O_4NiI_{0.52}$: C, 39.92; H, 2.96; N, 13.08; I, 15.40. Found: C, 37.60; H, 2.74; N, 13.07; I, 15.49.

The mass spectrum of the above crystals (10 or 70 eV, 200 °C source, 100 °C probe) exhibited a pattern characteristic of iodine and toluene.[16b]

Infrared data (Nujol mull, cm^{-1}): 3090 w, 1600 s, 1500 s, 1265 s, 1160 m, 1080 vs, 980 w (br), 830 m, 740 vs, 615 m.

Bis(benzoquinonedioximato)nickel·0.018iodine, $Ni(bqd)_2I_{0.018}$. A solution of $Ni(bqd)_2$ (6.2×10^{-3} M) and triply sublimed iodine (1.4×10^{-2} M) in benzene was heated to 78 °C and filtered while hot, and the filtrate was allowed to cool slowly to ambient temperature. The resulting dark crystals were collected by suction filtration, washed repeatedly with hexane, and dried in air. The crystals of this material are dark needles, exhibiting no golden luster. The C, H, N elemental analysis is experimentally indistinguishable from that of $Ni(bqd)_2$.

Anal. Calcd for $C_{12}H_{10}N_4O_4NiI_{0.018}$: C, 43.00; H, 3.01; N, 16.72. Found: C, 43.45; H, 3.25; N, 16.23. Calcd for $C_{12}H_{10}N_4O_4Ni$: C, 43.28; H, 3.03; N, 16.83.

A determination of the ratio of nickel to iodine in a single crystal (the X-ray data crystal) by neutron activation analysis gave Ni:I = 1.00:0.018(7).

Infrared data (Nujol mull, cm^{-1}): 3090 w, 1600 s, 1500 s, 1265 s, 1140 m, 1080 s, 950 s (br), 820 w, 740 vs, 610 m.

Spectral Measurements. Infrared, resonance Raman, and electronic spectra were recorded in the same manner and with the same apparatus as described previously.[3]

Iodine Mössbauer Studies. The apparatus and data acquisition/analysis procedures employed were as described previously.[3] Samples were prepared by weighing ca. 70 mg of $Ni(bqd)_2$ into a small vial, adding the desired amount of $^{129}I_2$[3] in 1-2 mL of benzene or o-dichlorobenzene, capping the vial, heating the mixture to ca. 80 °C, and then allowing it to cool slowly overnight. The solid product was next collected by centrifugation, washed several times with 1-2 mL of hexane, and then dried under a stream of dry nitrogen. Several samples were prepared which elemental analysis showed to have a Ni:I ratio greater than 1.0.

Single-Crystal Electron Transport Measurements. The procedures and apparatus for four-probe conductivity measurements were those described for the $M(dpg)_2I$ work.[3] Contact materials were colloidal graphite suspended in 1,3-butylene glycol or Demetron M8001 cold-setting conductive gold contact paint. Results with these two contact preparations were indistinguishable. Typical crystalline samples of the bisbenzoquinonedioximates were approximately tetragonal needles with lengths of 2.0-4.0 mm and widths of 0.1-0.3 mm. All measurements were conducted with current flow along the needle axis, i.e., along the molecular stacking direction. Variable-temperature studies employed measurements taken with both increasing and decreasing temperature to check for possible hysteresis; none was observed. Room temperature conductivity measurements were always made after high-temperature studies to ascertain if sample decomposition was taking place.

X-ray Diffraction Study of $Ni(bqd)_2I_{0.018}$. Preliminary film data were consistent with Laue symmetry *mmm*. Systematic extinctions are indicative of space groups *Ibam* or *Iba*2. Based on the setting angles of 14 manually centered reflections ($40° \leq 2\theta \leq 60°$, Cu $K\alpha_1$) the cell constants presented in Table I were obtained. Data were collected at room temperature on a Picker FACS-1 diffractometer using methods general in this laboratory.[17] Important features of the data collection are summarized in Table I.

The structure was solved and refined in a facile manner, using procedures and computer programs described before.[17] The centrosymmetric space group *Ibam* was assumed on the basis of excellent agreement among Friedel pairs. The positions of the atoms of the $Ni(bqd)_2$ species were obvious from a three-dimensional, origin-removed, sharpened Patterson function. Included in the final cycle of least-squares refinement were the contributions from hydrogen atoms on the carbon atoms. The positions of these hydrogen atoms were calculated, assuming C-H = 0.95 Å. The hydrogen atom position in the O(1)-H-O(2) hydrogen bond was not included. This final refinement converged to R indices and an error in an observation of unit weight given in Table I.

Examination of the final agreement between $|F_o|$ and $|F_c|$ reveals some disturbing features: (1) The highest residual peak of 1.36 e/Å^3 is located at ½00, but there is a general level of density along the ½0z line. (2) There are some outstanding differences between $|F_o|$ and $|F_c|$ especially for $hk0$ reflections (e.g., 510 (8.7, 25.0); 330 (12.3, 1.9 e$^-$)). On the basis of the neutron activation analysis of the data crystal (see above) there appears to be approximately 0.02 iodine atoms per nickel atom in the material. Presumably, the iodine atoms are positioned along the ½0z row, since there are large channels there that could accommodate iodine. Although a number of attempts were made to approximate the iodine scattering, none was especially successful. However, these calculations did establish that the overall structural parameters of the $Ni(bqd)_2$ portion of the structure are insensitive to models for the iodine scattering. Ultimately we chose as the final model one that ignores the presence of iodine. Table II presents the final parameters from this model. Table III presents the final listing of 10 $|F_o|$ vs. 10$|F_c|$ for those reflections used in the refinement.[18]

X-ray Diffraction Study of $Pd(bqd)_2I_{0.5}\cdot0.52C_6H_4Cl_2$. Preliminary film data indicated Laue symmetry 4/*mmm*, and systematic extinctions are consistent with space groups *P*4/*mcc* and *P*4*cc*. The cell constants (Table I) were obtained from the setting angles of 15 reflections manually centered on a FACS-1 diffractometer ($30 < 2\theta < 40°$, Mo $K\alpha_1$). Other features of the crystal and data collection are given in Table I.

The structure was solved and refined as described above. Examination of Friedel pairs strongly suggested that the centrosymmetric space group *P*4/*mcc* is the correct one. The $Pd(bqd)_2I_x$ portion of the structure was located from a Patterson function and subsequent difference Fourier maps. In the final refinement of this portion of the structure variable occupancy of the iodine atom was included. The resultant formula was $Pd(bqd)_2I_{0.444}$ and the final values of R, wR, and an error in an observation of unit weight were 0.070, 0.102, and

Table I. Crystal Data and Details of Data Collection and Structure Refinement

compd	$Ni(bqd)_2I_{0.018}$	$Pd(bqd)_2I_{0.48}$-$(C_6H_4Cl_2)_{0.91}$
formula	$C_{12}H_{10}I_{0.018}N_4NiO_4$	$C_{17.46}H_{13.64}Cl_{1.82}$-$I_{0.478}N_4O_4Pd$
formula weight, amu	355.16	575.07
a, Å	16.438 (5)	16.048 (7)
b, Å	14.759 (4)	16.048 (7)
c, Å	6.360 (2)	6.367 (3)
V, Å^3	1543.2	1639.6
space group	D_{2h}^{26} − *Ibam*	D_{4h}^{2}− *P*4/*mcc*
Z	4	4
ρ_{calcd}, g/cm^3	1.443	2.320
radiation	Cu $K\alpha$	Mo $K\alpha$
crystal shape	{001}{110} faces, needle axis [001]	{001}{110} faces, needle axis [001]
crystal dimensions, mm	0.8 × 0.1 × 0.1	0.8 × 0.2 × 0.2
crystal volume, mm^3	0.0062	0.030
μ, cm^{-1}	21.9	23.4
transmission factors	0.703-0.864	0.619-0.697
takeoff angle, deg	4.2	2.5
aperture, mm	5.5 × 4.8 32 cm from crystal	4.0 × 4.8 32 cm from crystal
scan speed, deg/min	2.0	2.0
scan range, deg	0.85 below $K\alpha_1$ to 0.85 above $K\alpha_2$	0.85 below $K\alpha_1$ to 0.85 above $K\alpha_2$
background counting times	20 s with rescan option	20 s with rescan option
2θ range	3-160°	3-80°
data collected	$h, k, \pm l$	$h \geq, k, l$ with l odd terminated at 55 ° $h \geq k, -l$ to 40°
p	0.04	0.03
unique data with $F_o^2 > 3\sigma(F_o^2)$	1026	1278
no. of variables	65	74
R index	0.11	0.052

3.63 e$^-$. Again there were some individual examples of poor agreement between $|F_o|$ and $|F_c|$, in this instance not restricted primarily to the $hk0$ reflections. A difference Fourier map showed as its main features a peak of height 1.28 e/Å^3 at approximately 0.06, 0.13, 0.15 and a ring of electron density about $x = 0$, $y = 0$ in the $z = ¼$ plane.

At this point it was discovered (see above) that the crystals of this compound contain varying amounts of o-dichlorobenzene, the average amount being 0.52 solvent molecule/palladium atom. Consequently, a number of attempts were made to account for the residual electron density as arising from a variable amount of o-$C_6H_4Cl_2$ in the 0,0, z channel. Because of the fourfold symmetry imposed on this channel and the fact that the solvent molecule does not intrinsically possess such symmetry, the disordering of the solvent is considerable. Although a calculation of the contributions of a $C_6H_4Cl_2$ rotor, constrained to lie in the $z = ¼$ plane, led to some improvement between $|F_o|$ and $|F_c|$, this model did not account for the main residual peak. Ultimately, a Cl atom was placed at the position of this residual peak and in subsequent cycles the occupancy and isotropic thermal parameter of this Cl atom were varied, along with the other variables of the $Pd(bqd)_2I_x$ portion. This refinement ultimately converged to the formula $Pd(bqd)_2I_{0.48}\cdot0.91$o-$C_6H_4Cl_2$ and agreement indices present in Table I. Because of correlation between occupancy and thermal parameter of the Cl atom and because of the very approximate nature of the model for solvent scattering, the ratio of solvent to $Pd(bqd)_2I$ derived from these data is very uncertain. We will henceforth refer to this compound, based upon the elemental analysis (vide supra), as $Pd(bqd)_2I_{0.50}0.52$-o-$C_6H_4Cl_2$. Placement of a Cl atom at this position is made chemically reasonable by the resultant Cl···Cl distance of 3.05 Å, a value to be expected in o-$C_6H_4Cl_2$. The improvement in agreement indices is considerable as is, more impor-

Table II. Positional and Thermal Parameters for the Atoms of $Ni(bqd)_2I_{0.018}$

ATOM	X^a	Y	Z	B11^b OR B, Å^2	B22	B33	B12	B13	B23
NI	0	0	0	4.09(11)	4.33(12)	22.86(79)	0.13(12)	0	0
O(1)	0.14497(63)	−0.09610(71)	0	5.44(44)	9.31(68)	32.6(30)	3.23(48)	0	0
O(2)	−0.02745(86)	0.18933(66)	0	9.87(68)	4.82(49)	38.1(34)	2.08(44)	0	0
N(1)	0.11201(62)	−0.01692(68)	0	3.46(33)	6.71(65)	25.6(29)	0.73(36)	0	0
N(2)	0.02939(93)	0.12475(78)	0	8.65(69)	4.75(55)	23.6(31)	−0.67(48)	0	0
C(1)	0.1547(83)	0.0605(11)	0	4.33(58)	10.9(11)	17.2(34)	−0.11(64)	0	0
C(2)	0.1005(10)	0.1430(10)	0	5.17(66)	6.91(76)	27.5(40)	−2.03(62)	0	0
C(3)	0.1423(15)	0.2287(13)	0	18.4(13)	7.0(12)	35.9(49)	−2.6(10)	0	0
C(4)	0.2275(23)	0.2243(28)	0	14.6(19)	25.5(32)	27.7(57)	−16.4(22)	0	0
C(5)	0.2801(15)	0.1446(29)	0	5.4(12)	24.0(34)	61.5(88)	−4.9(16)	0	0
C(6)	0.2487(11)	0.0640(19)	0	5.46(70)	18.0(21)	29.9(49)	−3.7(10)	0	0
H1C(3)	0.112	0.288	0	9.4					
H1C(4)	0.253	0.286	0	14.9					
H1C(5)	0.338	0.155	0	13.0					
H1C(6)	0.283	0.089	0	10.1					

^{a} Estimated standard deviations in the least significant figure(s) are given in parentheses in this and all subsequent tables. ^{b} The form of the anisotropic thermal ellipsoid is: $\exp[-(B11h^2 + B22k^2 + B33l + 2B12hk + 2B13hl + 2B23kl)]$. The quantities given in the table are the thermal cofficients × 10^3.

Table IV. Positional and Thermal Parameters for the Atoms of $Pd(bqd)_2I_{0.48}\cdot 0.91\,o\text{-}C_6H_4Cl_2$

ATOM	X^a	Y	Z	B11^b OR B, Å^2	B22	B33	B12	B13	B23
I	1/2	1/2	1/4	5.64(5)	5.64	54.53(63)	0	0	0
PD	0	1/2	0	3.83(3)	3.65(3)	15.44(14)	0.48(4)	0	0
O(1)	0.15758(34)	0.40918(34)	0	4.66(26)	4.81(27)	30.5(18)	1.79(23)	0	0
O(2)	0.98284(37)	0.68228(35)	0	7.38(38)	3.95(23)	35.6(19)	1.48(23)	0	0
N(1)	0.12319(41)	0.48284(4()	0	4.25(27)	5.74(40)	16.5(15)	0.76(23)	0	0
N(2)	0.03582(44)	0.61647(40)	0	5.32(31)	4.09(28)	18.8(17)	0.14(24)	0	0
C(1)	0.16713(54)	0.55317(53)	0	5.19(41)	5.49(43)	14.8(17)	−0.58(36)	0	0
C(2)	0.11747(54)	0.62895(52)	0	5.57(41)	4.86(38)	18.0(18)	−0.51(33)	0	0
C(3)	0.15949(69)	0.70790(62)	0	8.62(64)	5.69(49)	29.1(30)	−2.12(45)	0	0
C(4)	0.24404(83)	0.70553(92)	0	6.84(77)	9.22(75)	30.4(33)	−5.12(59)	0	0
C(5)	0.29217(64)	0.63317(96)	0	4.97(49)	12.34(92)	34.9(37)	−2.90(57)	0	0
C(6)	0.25675(53)	0.55806(75)	0	3.93(37)	9.49(64)	25.7(25)	−1.08(40)	0	0
H(3)	0.134	0.762	0	6.8					
H(4)	0.274	0.757	0	7.9					
H(5)	0.352	0.644	0	8.0					
H(6)	0.291	0.508	0	6.1					
H(O-O)	0.088	0.364	0	6.0					
CL	0.04858(96)	0.12534(77)	0.1431(18)	27.86(66)					

^{a} Estimated standard deviations in the least significant figure(s) are given in parentheses in this and all subsequent tables. ^{b} The quantities given in the table are the thermal cofficients × 10^3.

tantly, the removal of outstanding, individual discrepancies between $|F_o|$ and $|F_c|$. Table IV presents the final parameters from this model. Table V gives a listing of $10|F_o|$ vs. $10|F_c|$ for the reflections used in the refinement.[18]

Results and Discussion

Chemistry and Stoichiometry. The slow crystallization of $Ni(bqd)_2$ and $Pd(bqd)_2$ from certain hot aromatic solvents in the presence of an approximately tenfold molar excess of I_2 produces iodinated crystalline materials with a golden luster:

$$M(bqd)_2 + I_2 + S \rightleftharpoons M(bqd)_2{\cdot}I_x{\cdot}nS \qquad (1)$$
$$M = Ni, Pd$$
$$S = \text{aromatic solvent}$$

In the case of $Pd(bqd)_2$, iodination in o-dichlorobenzene yields a crystalline compound of approximate composition $Pd(bqd)_2I_{0.50}{\cdot}0.52\,o\text{-}C_6H_4Cl_2$. The presence of the solvent could be demonstrated by elemental analysis and mass spectrometry (see Experimental Section). $Ni(bqd)_2$ was found to be too soluble in o-dichlorobenzene to give good yields of a crystalline iodination product. However in toluene, golden, lustrous crystals of approximate composition $Ni(bqd)_2I_{0.52}{\cdot}0.32C_6H_5CH_3$ could be isolated. The solvent incorporation was again assigned by elemental analysis and mass spectrometry. For $Pd(bqd)_2$, the solubility in hot toluene was too small to allow isolation of crystalline iodinated materials in sufficient quantities for complete characterization. The above formulations differ from previous iodination studies on the nickel and palladium bisbenzoquinonedioximates where solvent incorporation (o-dichlorobenzene) was apparently not detected.[7,8,13] In our experiments, iodination of $Pd(bqd)_2$ in o-dichlorobenzene with a greater than tenfold excess of iodine produced a dark, flaky solid which analyzed approximately as $Pd(bqd)_2I_x$, $x = 1.5$–2.0. Iodination of $Ni(bqd)_2$ in hot benzene with a twofold excess of iodine yielded a dark (not golden) crystalline material which contained little or no iodine according to standard elemental analyses. For the crystal of this material chosen for X-ray diffraction studies (vide infra), neutron activation analysis revealed a nickel/iodine ratio consistent with the stoichiometry $Ni(bqd)_2I_{0.018}$. Thus, our chemical results indicate that the $M(bqd)_2I_x$ stoichiometry has considerably greater variability than previously thought, both in terms of halogen content and in terms of the tendency for solvent incorporation. It will be seen that both characteristics are understandable in terms of the crystal structures of these materials.

Resonance Raman and Iodine-129 Mössbauer Measurements. Raman spectra of the $M(bqd)_2I_x{\cdot}nS$ materials are presented in Figure 1; data are set out in Table VI. As was discussed in depth for the $M(dpg)_2I$ studies,[3] different polyiodide species give rise to characteristic, resonant-enhanced Raman scattering spectra.[5a,19] Spectra of $Ni(bqd)_2I_{0.52}{\cdot}0.32C_6H_5CH_3$ and $Pd(bqd)_2I_{0.50}{\cdot}0.52\,o\text{-}C_6H_4Cl_2$ are essentially identical; a strong emission is observed at 107 cm^{-1} and an overtone at 215 cm^{-1}. These bands are absent in the unio-

Table VI. Raman Data for Metal Bisbenzoquinonedioximates[a,b]

$Ni(bqd)_2$	none detected
$Ni(bqd)_2I_{0.018}$	none detected
$Ni(bqd)_2I_{0.52}\cdot 0.32C_6H_5CH_3$	322 w, 215 w, 153 w, 107 s
$Pd(bqd)_2$	none detected
$Pd(bqd)_2I_{0.5}\cdot 0.52o\text{-}C_6H_4Cl_2$	322 w, 215 m, 155 w, 107 s

[a] Polycrystalline samples, 5145 Å excitation. [b] In cm^{-1}; s = strong, m = medium, w = weak.

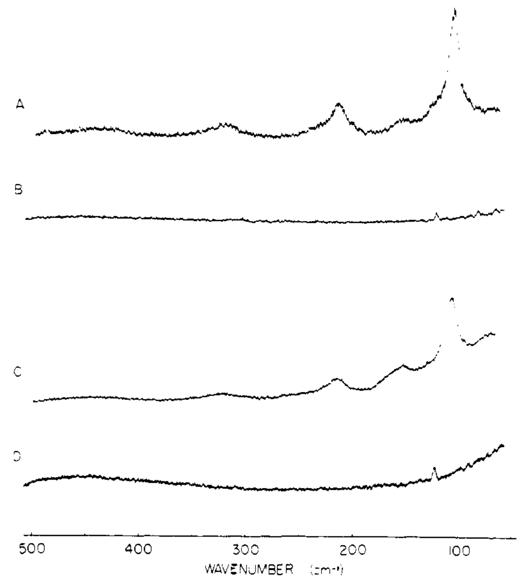

Figure 1. Resonance Raman spectra (ν_0 5145 Å) of (A) $Pd(bqd)_2I_{0.5}\cdot 0.52o\text{-}C_6H_4Cl_2$, (B) $Pd(bqd)_2$, (C) $Ni(bqd)_2I_{0.52}\cdot 0.32C_6H_5CH_3$, (D) $Ni(bqd)_2$. Weak transitions in (B) and (D) at 117 and 77 cm^{-1} result from laser plasma emission.

dinated materials. Such a Raman scattering pattern is characteristic of I_3^-, the 107-cm^{-1} vibration corresponding to the totally symmetric I-I-I stretch.[5a,19,20] There is no evidence for free I_2, weakly coordinated I_2, or any more than trace amounts of I_5^- in these spectra. As was discussed in the $M(dpg)_2I$ work, such species are readily detected in resonance Raman spectra.[3,5a,19] Unlike the diphenylglyoximate systems, no scattering from the $M(bqd)_2$ units could be discerned in the iodinated materials. In the iodine-rich compounds of stoichiometry $Pd(bqd)_2I_x$, x = 1.5–2.0, strong scattering at ca. 180 cm^{-1} was observed, indicative of weakly coordinated I_2, as found in the structures and spectra[5a,19] of materials containing I_2 and I_3^- units in close proximity (e.g., $(phenacetin)_2H^+I_3^-\cdot I_2$,[3,21a] $(Cs^+)_2(I_3^-)_2\cdot I_2$,[5a,19,21b] $(C_2H_5)_4N^+I_3^-\cdot 2I_2$[5a,10,21c]). In the iodine-poor material, $Ni(bqd)_2I_{0.018}$, no Raman scattering attributable to a polyiodide species could be observed. Control experiments indicated that this amount of iodine, present as I_3^- or I_5^-, would be detectable.

In an effort to explore the possibility that Raman-inactive I^- was present in the iodinated $M(bqd)_2$ materials, iodine-129 Mössbauer[22] studies[3,5a] were undertaken.[12] In a cubic or approximately cubic environment, I^- gives a characteristic singlet (δ −0.51 mm/s, e^2qQ = 0)[22] in the iodine Mössbauer spectrum. Because of the expense of iodine-129 and the very large excesses of iodine necessary to prepare practical quantities of $Ni(bqd)_2I_{0.52}\cdot 0.32C_6H_5CH_3$ or $Pd(bqd)_2I_{0.5}0.52o\text{-}C_6H_4Cl_2$ as crystalline samples, it was necessary to study polycrystalline powders. Several iodinated nickel specimens were prepared by stirring $Ni(bqd)_2$ compounds with a stoichiometric amount of $^{129}I_2$ in benzene or *o*-dichlorobenzene, then removing the supernatant and washing the solid product with hexane (see Experimental Section for details). The Raman spectra of these samples exhibited the characteristic I_3^- fundamental at ca. 108 cm^{-1} and no evidence of appreciable I_5^- or I_2. Elemental analysis showed a Ni:I ratio greater than 1.0. The Mössbauer spectra of these materials were somewhat broader than normal,[3] apparently reflecting macroscopic and microscopic sample inhomogeneity arising from the preparative procedure. For this reason the derived polyiodide spectral parameters are not as accurate as in the $M(dpg)_2I$ studies,[3] and exhaustive data refinement was not carried out. Most important, however, is the information these Mössbauer data provide on the possible presence of I^- or, also, free I_2 ($\delta \approx$ +0.98 mm/s, $e^2qQ \approx$ −1586 MHz).[22] A conservative estimate of the amount of I^- which could be present is 3 mol %; for free I_2, this number is ca. 5 mol %.

As already noted, an independent diffuse X-ray scattering study[13] of $Ni(bqd)_2I_{0.5}$ reached the same conclusion as our spectral studies in regard to the form of the iodine present: I_3^-. We find that the diffuse scattering pattern exhibited by $Pd(bqd)_2I_{0.50}\cdot 0.52o\text{-}C_6H_4Cl_2$ (vide infra) is identical with that of $Ni(bqd)_2I_{0.50}$,[13] indicating that an identical form of iodine is present, namely, I_3^-.

$Ni(bqd)_2I_{0.018}$ Crystal Structure. The crystal structure of $Ni(bqd)_2I_{0.018}$ is composed of individual $Ni(bqd)_2$ units which exhibit no unusual nonbonded contacts. The $Ni(bqd)_2$ units are stacked along the crystallographic *c* axis, such that the coordination planes of the Ni atoms are perpendicular to the stacking direction. A view of the unit cell is presented in Figure 2. Each $Ni(bqd)_2$ moiety is staggered by approximately 68° with respect to its nearest neighbors along the stacking axis.[23] The iodine atoms, whose presence was established by neutron activation analysis of the crystal used in the X-ray diffraction experiment, are presumed, based upon analogous structures, to be positioned in the channels[3,5a,7,8,13] along 1/2, 0, *z*, which exhibit residual electron density.

The Ni atoms in $Ni(bqd)_2I_{0.018}$ occupy the 4c special positions in the orthorhombic space group *Ibam*; thus, all Ni atoms are equally spaced along the stacking axis by *c*/2 (3.180 (2) Å). This Ni-Ni distance can be compared with values of 3.856 (2) Å for $Ni(bqd)_2$ (a monoclinic, slipped-stack structure)[9] and 3.153 (3) Å for $Ni(bqd)_2I_{0.50}$.[8] Partial oxidation typically results in a contraction in the metal-metal distance as illustrated by the nickel metallomacrocycles $Ni(dpg)_2$ and $Ni(dpg)_2I$ (3.547 Å vs. 3.271 (1) Å),[3] as well as NiPc[24] and NiPcI,[5a,e,f] Pc = phthalocyanine (4.79 Å for a slipped-stack structure vs. 3.244 (3) Å). Nickel-nickel separations for stacked, unoxidized glyoximate systems are as short as 3.24 Å in $Ni(CHD)_2$,[25] CHD = 1,2-cyclohexanedionedioximato, and 3.25 Å in $Ni(dmg)_2$,[26] dmg = dimethylglyoximato. The shortest Ni-Ni distances are found in the dimeric, eclipsed,

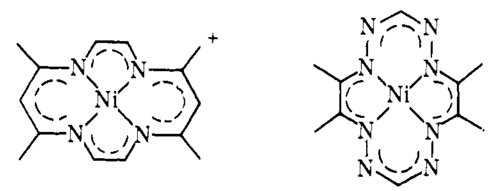

C D

face-to-face structures of nickel macrocyclic compounds C (Ni-Ni = 3.063 (1) Å)[27] and D (Ni-Ni = 2.788 (2) Å).[28] In these complexes the nickel atoms are displaced slightly out of the ligand planes (as defined by the four coordinated nitrogen atoms) toward each other. Thus, the interplanar spacings are estimated to be 3.19 (C)[27] and 3.00 Å (D).[28] The metal-metal separation in nickel metal is 2.49 Å.[29]

The $Ni(bqd)_2$ unit in $Ni(bqd)_2I_{0.018}$ has crystallographically imposed symmetry 2/*m* and is therefore planar. Figure 3 shows the structure of the molecule and the atom numbering scheme. The bond lengths and angles in the $Ni(bqd)_2$ unit are in good

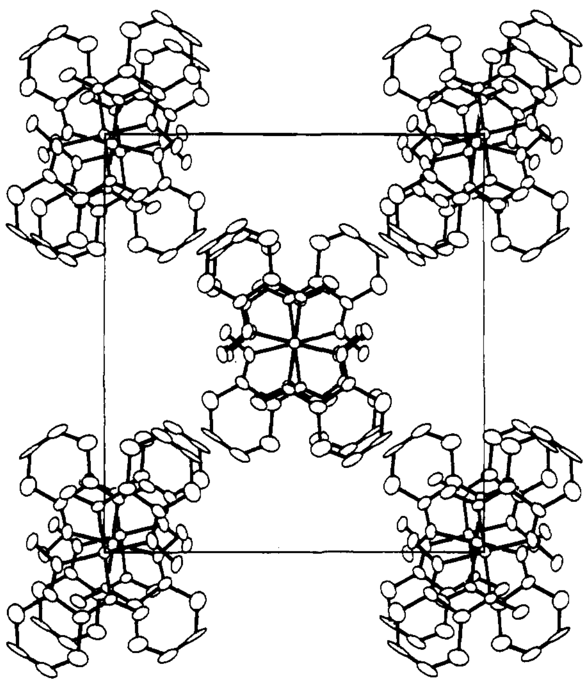

Figure 2. View of the unit cell of $Ni(bqd)_2I_{0.018}$ along the stacking direction. The *a* axis is vertical from botton to top, the *b* axis is horizontal to the right, and the *c* axis is toward the reader. The vibrational ellipsoids are drawn at the 50% level.

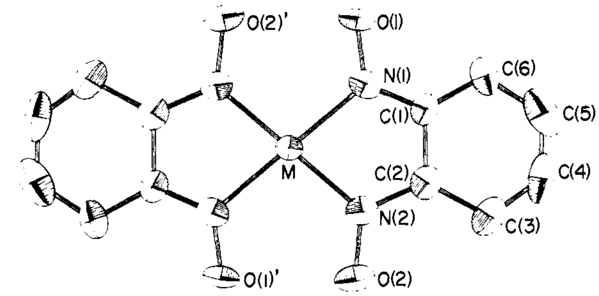

Figure 3. A drawing of the $Ni(bqd)_2$ molecule in $Ni(bqd)_2I_{0.018}$ showing the atom numbering scheme. The vibrational ellipsoids are drawn at the 50% level.

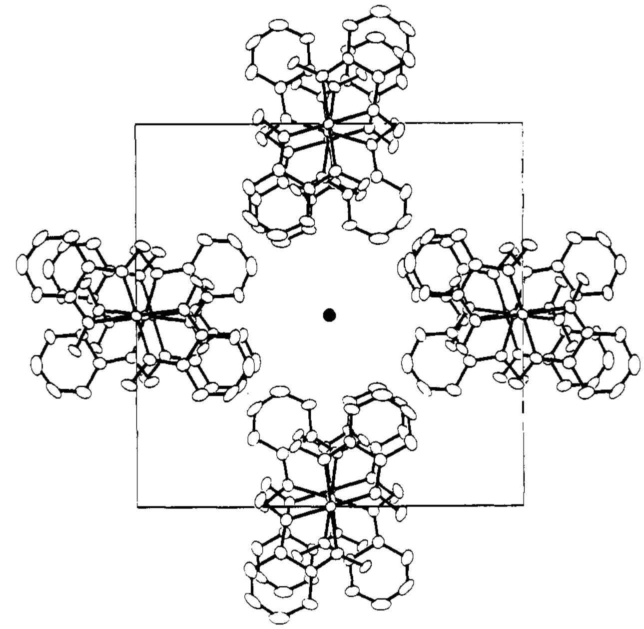

Figure 4. View of the unit cell of $Pd(bqd)_2I_{0.5}\cdot 0.52o\text{-}C_6H_4Cl_2$ along the stacking direction. The *a* and *b* axes are in the plane of the page, and the *c* axis is toward the reader. The vibrational ellipsoids are drawn at the 50% level; the dark circle depicts an iodine atom.

agreement with the parameters reported in $Ni(bqd)_2$[9] and $Ni(bqd)_2I_{0.5}$.[8] These values are set out in Table VII.

$Pd(bqd)_2I_{0.5}\cdot 0.52o\text{-}C_6H_4Cl_2$ Crystal Structure. The structure of $Pd(bqd)_2I_{0.5}\cdot 0.52o\text{-}C_6H_4Cl_2$ is composed of individual $Pd(bqd)_2$ units and I atoms exhibiting no unusual nonbonded contacts. A view of the unit cell is presented in Figure 4. The $Pd(bqd)_2$ moieties are stacked along the crystallographic *c* axis, such that the coordination planes of the Pd atoms are perpendicular to the stacking direction. Each $Pd(bqd)_2$ moiety is staggered by approximately 65° with respect to its nearest neighbors along the stacking axis. The iodine atoms also stack one above the other in the *c* direction, filling the "tunnels" along $\frac{1}{2}\frac{1}{2}z$ created by the benzo rings of the benzoquinonedioximato ligands. The observed diffuse X-ray scattering pattern, which is identical with that reported for $Ni(bqd)_2I_{0.5}$,[13] is attributable to the disorder of the iodine atoms along the stacking direction. In addition, the *o*-dichlorobenzene molecules are believed to reside, in a disordered fashion, in the tunnels of larger diameter (along 00*z*) created by the oxygen atoms and benzo rings of the benzoquinonedioximato ligands.

The Pd atoms occupy the 4f special positions in the space group *P4/mcc*; thus, all Pd atoms are equally spaced along the stacking direction by $c/2$ (3.184 (3) Å). This Pd–Pd distance is comparable with the Pd–Pd distances found in the partially oxidized stacked glyoximate compounds $Pd(gly)_2I$ (3.244 (1) Å),[30] gly = glyoximato, and $Pd(dpg)_2I$ (3.26 Å).[31a,b] These distances are significantly shorter than the Pd–Pd distances found in the corresponding precursors $Pd(gly)_2$ (3.558 Å)[32] and $Pd(dpg)_2$ (3.52 Å)[31c] but are only slightly shorter than the Pd–Pd distances in the unoxidized complexes $Pd(bqd)_2$ (3.202 (1) Å),[10] $Pd(dmg)_2$ (3.253 Å),[26] and $Pd(CHD)_2$ (3.250 Å).[25] All of the above distances are considerably longer than the metal–metal distance in palladium metal (2.75 Å).[29]

The $Pd(bqd)_2$ unit has crystallographically imposed symmetry $2/m$ and is required to be planar. The molecular geometry is essentially that shown for $Ni(bqd)_2I_{0.018}$ in Figure 3; the atom numbering scheme is the same. The bond lengths and angles in the $Pd(bqd)_2$ unit of the $Pd(bqd)_2I_{0.5}\cdot 0.52o\text{-}C_6H_4Cl_2$ crystal structure are in good agreement with the parameters reported in $Pd(bqd)_2$,[10] and these values are given in Table VII. The most significant differences in the parameters of the $Pd(bqd)_2$ units in the two structures are in the Pd–N(1)–C(1) and Pd–N(2)–C(2) bond angles, 114.0 (6) and 115.8 (6)° in $Pd(bqd)_2I_{0.5}\cdot 0.52o\text{-}C_6H_4Cl_2$ and 122 (1) and 124 (1)° in $Pd(bqd)_2$.[10]

Electronic Spectra. Figure 5 presents electronic spectra of the $M(bqd)_2$ and $M(bqd)_2I_x$ compounds as polycrystalline speciments. Data are compiled in Table VIII. Several features are noteworthy. For both nickel and palladium systems, iodination does not produce a detectable change in the spectra at wavelengths shorter than ca. 500 nm. Considering the drastic structural change which occurs upon iodination of $Ni(bqd)_2$ (monoclinic slipped stack structure with Ni–Ni = 3.856 (2) Å[9] → tetragonal stacked structure with Ni–Ni = 3.153 (3) Å[8]) it seems unlikely that these bands are metal–metal[3] (intramolecular $nd_{z^2} \rightarrow (n+1)p_z$ transitions with borrowing of intensity from metal → metal charge transfer transitions[33]) in origin. Rather, these are, in all likelihood, $M(bqd)_2$ molecular transitions. The second noteworthy feature of the electronic spectra is the appearance of a broad transition in the 600-nm region upon iodination. We assign a major part of this absorption to the I_3^- chains. As discussed elsewhere, such intense optical transitions are typical of delocalized polyiodides.[3,34] The spectrum of $(benzamide)_2H^+I_3^-$, which

Table VII. Comparison of Bond Distances (Å) and Angles (deg) in Nickel and Palladium Bisbenzoquinonedioximates[a]

	$Ni(bqd)_2I_{0.018}$[b]	$Ni(bqd)_2I_{0.5}$[c]	$Ni(bqd)_2$[d]	$Pd(bqd)_2I_{0.5}\cdot 0.52C_6H_4Cl_2$[e]	$Pd(bqd)_2$[f]
M-M	3.180 (1)	3.153 (3)	3.856 (2)	3.183 (2)	3.202 (1)
M-N(1)	1.858 (10)	1.91 (2)	1.868 (4)	1.996 (7)	2.00 (2)
N(1)-N(2)	1.904 (10)	1.90 (2)	1.860 (5)	1.955 (7)	1.95 (2)
M-O(1)	1.288 (12)	1.33 (3)	1.313 (7)	1.305 (7)	1.34 (2)
N(2)-O(2)	1.335 (16)	1.28 (3)	1.313 (8)	1.356 (8)	1.33 (3)
N(1)-C(1)	1.341 (17)	1.27 (4)	1.309 (8)	1.331 (10)	1.29 (3)
N(2)-C(2)	1.199 (20)	1.35 (4)	1.313 (8)	1.325 (10)	1.35 (3)
C(1)-C(2)	1.510 (22)	1.50 (4)	1.445 (8)	1.454 (11)	1.47 (3)
C(1)-C(6)	1.545 (20)	1.44 (4)	1.424 (8)	1.441 (12)	1.43 (3)
C(2)-C(3)	1.440 (21)	1.42 (4)	1.427 (9)	1.435 (12)	1.43 (3)
C(3)-C(4)	1.402 (46)	1.42 (6)	1.346 (10)	1.358 (15)	1.38 (4)
C(4)-C(5)	1.460 (45)	1.42 (7)	1.432 (11)	1.395 (18)	1.48 (4)
C(5)-C(6)	1.297 (38)	1.32 (6)	1.338 (11)	1.333 (15)	1.34 (4)
O(1)-O(2)	2.372 (17)	2.43 (3)	2.480 (6)	2.687 (9)	2.66 (4)
N(1)-M-N(2)	83.0 (5)	84 (1)	83.6 (2)	80.8 (3)	81 (1)
O(1)-N(1)-C(1)	123.5 (11)	122 (2)	124.9 (4)	123.0 (7)	124 (2)
O(2)-N(2)-C(2)	121.4 (14)	122 (2)	125.7 (4)	120.1 (7)	120 (2)
C(1)-C(2)-C(3)	115.2 (16)	122 (3)	119.1 (5)	118.7 (8)	121 (2)
C(2)-C(3)-C(4)	129.0 (23)	112 (2)	118.6 (6)	116.4 (11)	119 (2)
C(3)-C(4)-C(5)	120.2 (23)	129 (4)	122. 1 (7)	125.2 (11)	120 (3)
C(4)-C(5)-C(6)	115.4 (25)	120 (4)	121. 5 (7)	121.1 (10)	123 (3)
C(5)-C(6)-C(1)	124.3 (16)	119 (3)	117.0 (6)	118.4 (10)	120 (2)
C(6)-C(1)-C(2)	113.9 (9)	119 (3)	119.8 (6)	120.1 (8)	117 (2)
M-N(1)-C(1)	113.9 (9)	115 (2)	115.4 (4)	114.0 (6)	122 (1)
M-N(2)-C(2)	117.7 (12)	113 (2)	114.7 (4)	115.8 (6)	124 (1)

[a] Atom numbering scheme is that in Figure 3. [b] This work. [c] Reference 8 and the refinement described in this work. [d] Reference 9. [e] This work. [f] Reference 10.

Table VIII. Electronic Spectral Data for Metal Bisbenzoquinonedioximates in nm ($\times 10^3$ cm^{-1})[a,b]

compd	Nujol mull		$CHCl_3$ solution	
$Ni(bqd)_2$	238	(42.0)		
	318	(31.4)	308	(32.5)
	420 sh	(23.8)	417	(24.0)
	472	(21.2)	455	(22.0)
	590	(16.9)	553 sh	(18.1)
$Ni(bqd)_2I_{0.52}\cdot 0.32C_6H_5CH_3$	220 sh	(45.5)		
	260	(38.5)		
	315	(31.7)		
	450	(22.2)		
	540	(18.5)		
	650 br	(15.4)		
	802	(12.5)		
$Pd(bqd)_2$	235	(42.6)		
	295 sh	(33.9)		
	325 sh	(30.8)	335	(29.8)
	385	(26.0)	393	(25.4)
	440 sh	(22.7)	505 sh	(19.8)
	680	(14.7)	650 br	(15.4)
$Pd(bqd)_2I_{0.5}\cdot 0.52o\text{-}C_6H_4Cl_2$	295 sh	(33.9)		
	320 sh	(31.2)		
	390	(25.6)		
	440 sh	(22.7)		
	605 sh	(16.5)		
	685 br	(14.6)		

[a] sh = shoulder, br = broad. [b] Data in parentheses given in cm^{-1}.

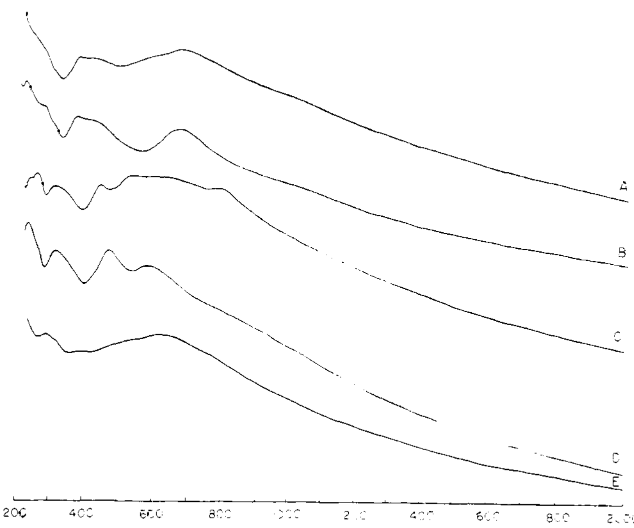

Figure 5. Electronic spectra (Nujol mulls) of polycrystalline samples of (A) $Pd(bqd)_2I_{0.5}\cdot 0.52o\text{-}C_6H_4Cl_2$, (B) $Pd(bqd)_2$, (C) $Ni(bdq)_2I_{0.52}\cdot 0.32C_6H_5CH_3$, (D) $Ni(bqd)_2$, (E) $(benzamide)_2H^+I_3^-$.

is also a triiodide chain compound,[35] is presented in Figure 5 for comparison. A recent polarized single crystal reflectance study[14] of $Ni(bqd)_2I_{0.50}$ and $Pd(bqd)_2I_{0.50}$ reached the conclusion that reflectance maxima at 1.6–1.7 eV (775–730 nm)[36] in these materials, which were polarized in the chain direction, were metal-metal (d_{z^2} band $\rightarrow$ p_z band) in origin. Although such an assignment for the $M(bqd)_2$ stacks is reasonable, it must be noted that the intense polyiodide transition should also be polarized in the chain direction[34c] and that the presence of the I_3^- chains cannot be ignored in such analyses.

Comparison of Metal Bisbenzoquinonedioximate Crystal Structures. The metrical and oxidation state information contributed by the present investigation now allows a detailed assessment of the crystal structural consequences of partial oxidation. A comparison of unit cell data for the series is compiled in Table IX; bond distances and angles are set out in Table VII. In the nickel system, the unoxidized material, $Ni(bqd)_2$, has a slipped-stack structure.[9] A packing diagram, which has not previously been shown, is presented in Figure 6. As has been noted elsewhere,[8,13] this arrangement of the planar molecules within the unit cell allows more efficient packing (as judged by the density) than a stacked arrangement

Table IX. Comparison of Unit Cell Parameters for Various Metal Benzoquinonedioximates

	a	*b*	*c*	*d*	
compd	$Ni(bqd)_2$	$Ni(bqd)_2I_{0.018}$	$Ni(bqd)_2I_{0.50}$	$Pd(bqd)_2$	$Pd(bqd)_2I_{0.5}$
space group	C_{2h}^5-$P2_1/n$	D_{2h}^{26}-$Ibam$	D_{4h}^2-$P4/mcc$	D_{2h}^{26}-$Imcb$	D_{4h}^2-$P4/mcc$
Z	2	4	4	4	4
a, Å	3.856 (3)	16.438 (2)	15.553 (4)	6.405 (1)	16.048 (7)
b, Å	9.461 (6)	14.759 (4)	15.553 (4)	9.728 (1)	16.048 (7)
c, Å	16.542 (12)	6.360 (2)	6.307 (3)	20.649 (2)	6.367 (3)
β, deg	90.45 (6)	90	90	90	90
V, Å^3	603.5	1543.2	1525.6	1286	1639.6
symmetry imposed on $M(bqd)_2$	$\bar{1}$	$2/m$	$2/m$	$2/m$	$2/m$

[a] Reference 9. [b] This work. [c] Reference 8. [d] Reference 10.

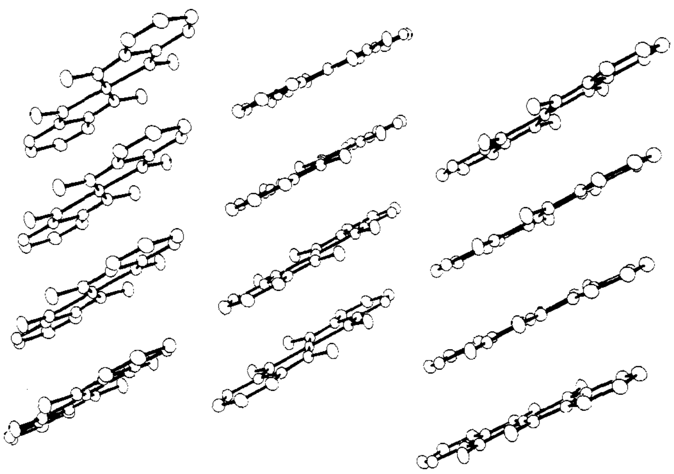

Figure 6. Packing diagram of $Ni(bqd)_2$ plotted from the data of ref 9. Vibrational ellipsoids are drawn at the 50% level.

where the molecular planes are perpendicular to the stacking direction. In contrast to the $Ni(bqd)_2$ result, the $Ni(bqd)_2I_{0.018}$ structure is an orthorhombic stacked one. Figure 7 compares the packing of stacked $M(bqd)_2I_x$ structures. The change in crystal structure on proceeding from $Ni(bqd)_2$ to $Ni(bqd)_2I_{0.018}$ includes a decrease in the interplanar spacing of 0.22 Å and a decrease in the metal–metal distance of 0.68 Å. There is no significant alteration in metrical parameters within the $Ni(bqd)_2$ unit (Table VII). The crystal structure of $Ni(bqd)_2I_{0.018}$ evidences large tunnels extending in the stacking direction which contain only a small amount of iodine, but which may have contained larger quantities of material at some time during the crystallization process. That polyiodide species (I_2, I_3^-, etc.) were not detected in the resonance Raman examination of this material suggests the predominant presence of iodine as I^- and that the solid-state charge distribution can be formally represented as $Ni(bqd)_2{}^{0.018+}(I^-)_{0.018}$. The presence of undetected polyiodides (e.g., I_3^-) would mean that the degree of partial oxidation was even lower. Further oxidation of $Ni(bqd)_2$ produces "$Ni(bqd)_2I_{0.50}$" with iodine present predominantly as I_3^-, indicating a formal charge distribution of $Ni(bqd)_2{}^{0.17+}(I_3^-)_{0.50/3}$. The oxidation state change is accompanied by an additional 0.027-Å contraction in the Ni–Ni distance. There is no perceptible change in the internal $Ni(bqd)_2$ dimensions. Interestingly, the angle of eclipsing between $Ni(bqd)_2$ units changes only slightly upon further oxidation (68° → 65°); however, the relative orientation of the stacks changes appreciably. As can be seen in Figure 7, the effect is to provide two sets of tunnels which are nonequivalent in size and in surrounding environment. The smaller tunnel, which contains the iodine, is of approximate cross-sectional dimensions 4.8 × 4.8 Å and is lined with hydrophobic C–H residues. The larger tunnel is ca. 7.4 × 7.4 Å in size and is surrounded by C–H groups as well as more polar oxygen atoms which are engaged in hydrogen bonding). These tunnels contain the solvent molecules. In contrast to this result, the tunnels in $Ni(bqd)_2I_{0.018}$ are all crystallographically equivalent, have both polar and nonpolar regions, and differ in size (ca. 5 × 6 Å) from those in $Ni(bqd)_2I_{0.50}$.

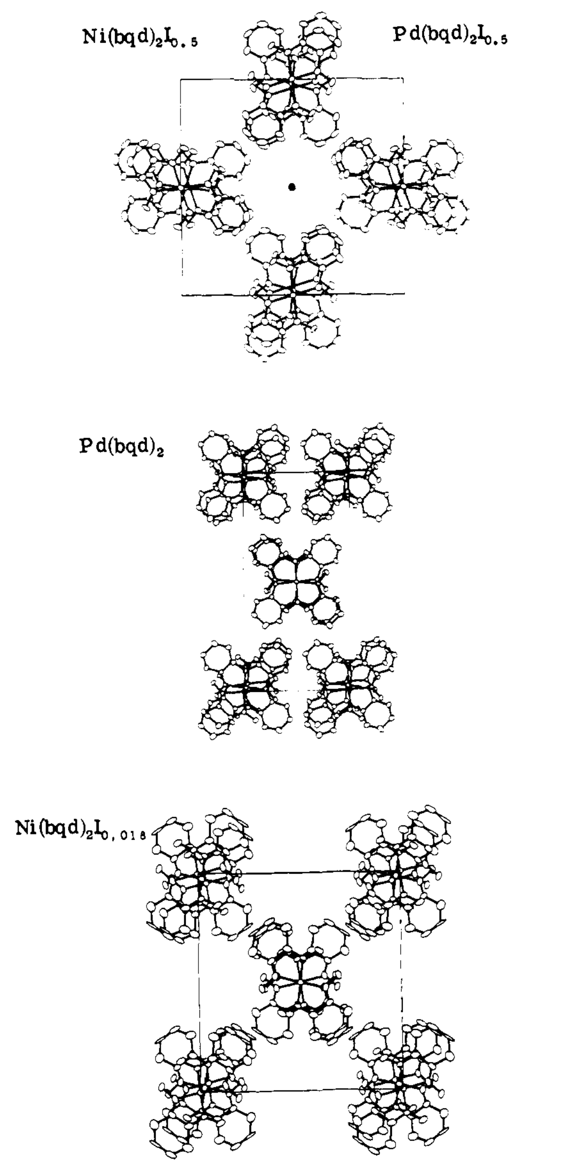

Figure 7. Comparison of metal bisbenzoquinonedioximate crystal structures viewed along the stacking direction.

The structure of $Pd(bqd)_2$ is orthorhombic with molecular planes perpendicular to the stacking direction and a 90° eclipsing angle between neighboring $Pd(bqd)_2$ units (Figure 7). The degree to which this structure differs from that of

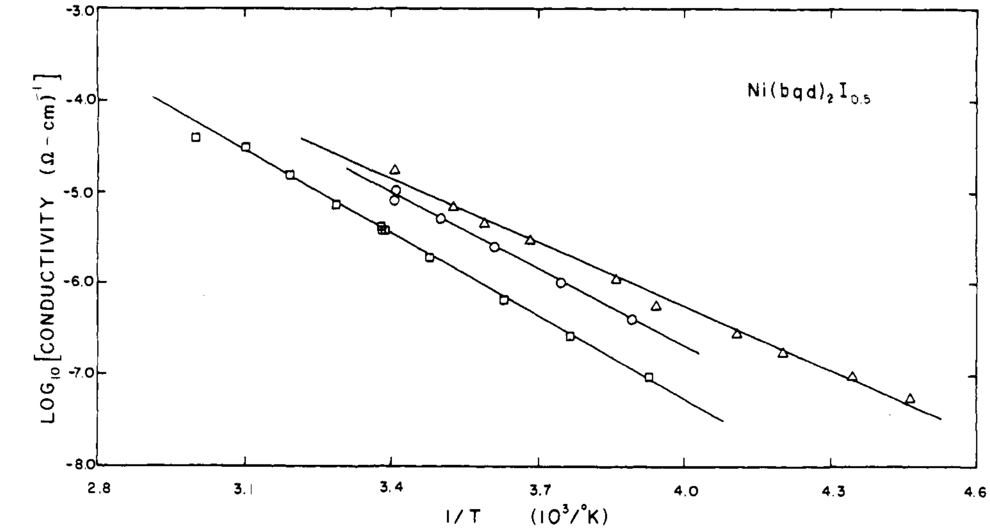

Figure 8. Electrical conductivity (dc) of representative $Ni(bdq)_2I_{0.52}{\cdot}0.32CH_3C_6H_5$ crystals as a function of temperature. Data are measured in the crystallographic *c* direction.

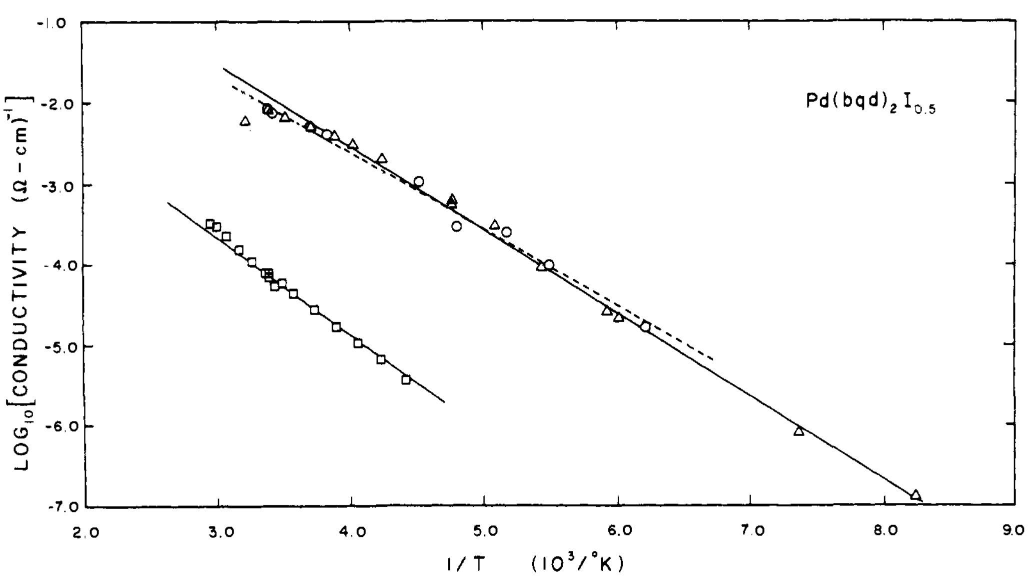

Figure 9. Electrical conductivity (dc) in the crystallographic *c* direction of representative $Pd(bqd)_2I_{0.5}{\cdot}0.52o\text{-}C_6H_4Cl_2$ crystals as a function of temperature.

monoclinic $Ni(bqd)_2$ may not be energetically significant since there is evidence[14] (as yet unpublished) that $Pd(bqd)_2$ can also be crystallized in the same monoclinic form observed for $Ni(bqd)_2$. Upon partial oxidation to $Pd(bqd)_2^{0.17+}(I_3^-)_{0.50/3}$, the Pd–Pd distance decreases by 0.019 Å and the eclipsing angle between the stacked metallomacrocycle moieties decreases by 25°. A spreading out of the structure in the *a-b* plane provides tunnels for iodine and solvent inclusion. The arrangement of groups within the unit cell of $Pd(bqd)_2I_{0.5}{\cdot}0.52o\text{-}C_6H_4Cl_2$ is identical with that in $Ni(bqd)_2I_{0.50}$. Indeed, our refinement of the published $Ni(bqd)_2I_{0.50}$ crystallographic data,[8] reported for a crystal grown from *o*-dichlorobenzene,[8] indicates residual electron density in the larger set of lattice tunnels, i.e., those which contain solvent in $Pd(bqd)_2I_{0.5}{\cdot}0.52o\text{-}C_6H_4Cl_2$. The internal structural parameters of the $Pd(bqd)_2$ unit change insignificantly upon partial oxidation (Table VII).

Electrical Conductivity. Four-probe, variable-temperature *c*-axis conductivity data for $Ni(bqd)_2I_{0.52}{\cdot}0.32C_6H_5CH_3$ and $Pd(bqd)_2I_{0.5}{\cdot}0.52o\text{-}C_6H_4Cl_2$ single crystals are shown in Figures 8 and 9, respectively. These and related data are summarized in Table X. The range of conductivities observed for the $Ni(bqd)_2I_{0.52}{\cdot}0.32C_6H_5CH_3$ crystals is fairly narrow for all samples examined. The wider range for the $Pd(bqd)_2I_{0.5}{\cdot}0.52o\text{-}C_6H_4Cl_2$ data includes a single sample of particularly poor conductivity. Nearly all other values were clustered at the high conductivity end of the range. Table X also compares the dc conductivity of selected $M(bqd)_2I_{0.5}{\cdot}S$ crystals with measurements at a frequency of 100 Hz. For M = Pd, there is good agreement between the techniques. For M = Ni, there is less good agreement, which is attributed to the integrity of the electrode contacts. The nickel-containing specimens presented the greatest measurement difficulties, and a large number of crystals were rejected owing to fractures and to nonohmic electrode behavior.

It can be seen in Table X that the conductivities of the uniodinated $M(bqd)_2$ materials are immeasurably low. As has been observed for the metal bisdiphenylglyoximates and similar macrocycles, partial oxidation such as to $M(bqd)_2^{0.17+}$ results in a large increase in electrical conductivity. The enhancement for the bisbenzoquinonedioximates is ca. 10^3–10^6. Interestingly, considerably lower conductivities are observed for the $Ni(bqd)_2I_{0.018}$ crystals than for the $Ni(bqd)_2I_{0.52}{\cdot}0.32C_6H_5CH_3$ crystals. This may reflect the differences in

Table X. Single Crystal (c axis) Electrical Conductivity Data for Metal Bisbenzoquinonedioximates and Bisdiphenylglyoximates

material	dc conductivity[c] at 300 K, $(\Omega\ cm)^{-1}$	conductivity comparison at 300 K, $(\Omega\ cm)^{-1}$ [e] dc	ac (100 Hz)	Δ, eV[f]	L, Å[g]
$Ni(bqd)_2$	$<9 \times 10^{-9}$				
$Ni(bqd)_2I_{0.018}$	$<9 \times 10^{-9}$				$<7.0 \times 10^{-13}$
$Ni(bqd)_2I_{0.52}{\cdot}S$[a]	$1.8–11 \times 10^{-6}$	1.8×10^{-6}	1.1×10^{-7}	0.54 ± 0.08	$1.4–8.6 \times 10^{-8}$
$Pd(bqd)_2$	$<2 \times 10^{-9}$				
$Pd(bqd)_2I_{0.5}{\cdot}S$[b]	$7.8–810 \times 10^{-5}$	5.6×10^{-3}	4.5×10^{-3}	0.22 ± 0.03	$6.4–670 \times 10^{-7}$
$Ni(dpg)_2I$	$2.3–11 \times 10^{-2}$			0.19 ± 0.01	$4.0–20 \times 10^{-4}$ [d]
$Pd(dpg)_2I$	$7.7–47 \times 10^{-4}$			0.54 ± 0.11	$1.3–8.0 \times 10^{-5}$ [d]

[a] S = 0.32 toluene. [b] S = 0.52o-dichlorobenzene. [c] Range for crystals examined. [d] From ref 3. [e] Data for the same crystal. [f] From least-squares fit to the equation $\sigma e^{-\Delta/kT}$. [g] From the relationship $L = \pi h\sigma/2e^2N$.

crystal structure as well as the decreased number of charge carriers generated by the smaller degree of partial oxidation. In the only other case to date where it has been possible to vary the apparent degree of metallomacrocycle oxidation, i.e., $Ni(OMTBP)I_x$, OMTBP = octamethyltetrabenzoporphyrin, x = 1.084 (4) and 2.9 (3) (iodine present as I_3^-),[37] the x = 2.9 materials appear to be slightly less conductive. The difference is not nearly so large as in the present case.

The dc conductivities of the $M(bqd)_2I_{0.50}{\cdot}S$ materials obey the equation

$$\sigma = \sigma_0 e^{-\Delta/kT} \qquad (2)$$

where Δ is the apparent activation energy, over the range of temperatures shown in Figures 8 and 9. The $M(dpg)_2I$ compounds exhibit similar behavior.[3] At the highest temperatures some $M(bqd)_2I_{0.50}{\cdot}S$ samples did display a tendency toward leveling off in the ln σ vs. $1/T$ plot. Efforts to confirm "metal-like" behavior, i.e., decreasing conductivity with increasing temperature, by acquiring additional data at even higher temperatures resulted in irreversible sample decomposition. Table X contains apparent activation energies, Δ, obtained by a least-squares fit to eq 2. The range indicated represents the largest deviation from the average for the samples plotted. As was noted in the discussion of the $M(dpg)_2I$ conductivity data,[3] the thermally activated temperature dependence of charge transport in these materials is consistent with either of two theoretical descriptions: phonon-assisted carrier hopping between states localized by static disorder,[38] or an activated carrier concentration in a system with a Mott–Hubbard or some other type of gap.[39] For the former model the disorder in the I_3^- chains would presumably be the source of the disorder, while for the latter model the classical Mott–Hubbard gap[38d,39b] is inappropriate for the $M(bqd)_2I_{0.50}{\cdot}S$ bands, which are ca. 92% filled.

Table X also compares the $M(bqd)_2I_{0.5}{\cdot}S$ conductivity data with those for $M(dpg)_2I$ materials. Even after adjusting the transport behavior for crystal structure by considering the carrier mean free path, L:

$$L = \frac{\pi h \sigma}{2e^2 N} \qquad (3)$$

which is a function of the number of conducting chains per cross-sectional area (N), it can be seen that that the bisbenzoquinonedioximate materials are less conductive. Apparent activation energies are, however, more comparable (Table X), and in each bisglyoximate series the Δ values for the highest conductor and lowest conductor are similar.

Conclusions

The results of the present investigation indicate that the $M(bqd)_2I_{0.50}$ materials, M = Ni, Pd, are best formulated as $M(bqd)_2I_{0.50}{\cdot}S$ materials where S represents various amounts of the aromatic solvent employed for crystallization. As deduced from resonance Raman, ^{129}I Mössbauer, and diffuse X-ray scattering measurements,[13] the iodine is present as I_3^-, and thus the $M(bqd)_2I_{0.50}{\cdot}S$ materials are indeed partially oxidized. The formal fractional charge on the $M(bqd)_2$ is +0.17. Based upon estimated uncertainties in stoichiometry and I_3^- content we assign to this oxidation state an uncertainty of 0.02 charge units. It is interesting to note that the degree of charge transferred in the present case is identical, within experimental error, to that deduced in the bisdiphenylglyoximate materials, $M(dpg)_2I$, M = Ni, Pd. Here iodine was present predominantly as I_5^- so that the formal oxidation of each $M(dpg)_2$ moiety was +0.20 (4).[3]

In both benzoquinonedioximate and diphenylglyoximate systems, partial oxidation is accompanied by contraction in the interplanar stacking distances. The shortest metal–metal distance observed for a stacked, partially oxidized metal bisdioximate is 3.153 (3) Å in $Ni(bqd)_2I_{0.50}$, with the distance in $Pd(bqd)_2I_{0.5}{\cdot}0.52o\text{-}C_6H_4Cl_2$ being only slightly longer, i.e., 3.184 (3) Å. Contacts in the $M(dpg)_2I$ species are somewhat longer with Ni–Ni = 3.271 (1) Å and Pd–Pd = 3.25 Å.[3] These metal–metal distances are greater than in $K_2Pt(CN)_4Br_{0.30}$ (2.89 Å)[4,40] as well as in the integral oxidation state face-to-face metallomacrocycle dimers $[Ni(C_{14}H_{18}N_4)]_2^{2+}$ (C, Ni–Ni = 3.063 (1) Å)[27] and $[Ni(C_{18}H_{14}N_8)]_2$ (D, Ni–Ni = 2.788 (2) Å).[28] However, since the nickel atoms in the latter two compounds are significantly displaced from the ligand planes[41] (and toward each other) it is more meaningful to discuss the interplanar spacing. This value for C is 3.19 Å, and for D is 3.00 Å, which is in better agreement with the stacked bisdioximate parameters. The attractive forces in the face-to-face dimers are considered to involve both metal–metal σ and δ bonding as well as ligand–ligand π bonding.[27,28] It is likely that similar effects are operative in the stacked bisdioximates, with the result of partial oxidation being to depopulate orbitals (bands) which are metal–metal (e.g., nd_{z^2}[42]) or ligand–ligand antibonding[43] in character. The lengths of the Ni–Ni and Pd–Pd contacts as well as the relative insensitivity of the stacking distances to metal identity suggests that the metal–metal bonding is rather weak. That the interactions do not persist in solution indicates that the overall attractive forces are not very great. As a point of reference, the interplanar spacing in Ni(Pc)I is 3.244 (3) Å,[5f] in graphite it is 3.35 Å,[44] and in the TCNQ stacks of typical organic conductors it is 3.17–3.30 Å.[45] In the absence of some attractive forces, distances in the 3.0-Å range are considered to be moderately repulsive.[46]

Partial oxidation of the $M(bqd)_2$ and $M(dpg)_2$ materials to the 0.17–0.20 formal oxidation state results in an electrical conductivity increase of 10^3–10^8 in the molecular stacking direction. For $Ni(bqd)_2I_{0.018}$ the small degree of oxidation results in a greatly diminished electrical conductivity compared with $Ni(bqd)I_{0.52}{\cdot}0.32C_6H_5CH_3$. For the partially oxidized $M(bqd)_2$ and $M(dpg)_2$ materials, there is no clear-cut dependence of the charge transport facility on metal or interplanar spacing. The approximate order of conductivity is

$Ni(dpg)_2I > Pd(dpg)_2I \approx Pd(bqd)_2I_{0.50}{\cdot}S > Ni(bqd)_2I_{0.50}{\cdot}S$. There is no evidence in the present case that the chains of metal atoms provide the major conductive pathway, and judging from results on macrocyclic systems (phthalocyanine,[5b] dibenzotetraazaannulene[5c]) where both metal and metal-free species are conductive when partially oxidized, it is likely that the ligand (i.e., molecular orbitals which are largely ligand in character) plays an important if not predominant role in the conductivity of the bisdioximate materials. The temperature dependence of the conductivity in the present materials is thermally activated with slight, if any, onset of "metal-like" behavior at highest temperatures. The functional dependence is reminiscent of "intermediate conductivity" TCNQ salts,[45b] and is consistent with phonon-assisted hopping of the carriers between states localized by disorder,[38] or with a weakly localized system having a gap and a temperature-dependent carrier concentration.[39]

Acknowledgments. This work was generously supported under the NSF-MRL program through the Materials Research Center of Northwestern University (Grant DMR76-80847), by the Office of Naval Research (T.J.M.), the Department of Energy (S.L.R), and the National Science Foundation (Grant CHE76-10335 to J.A.I.).

Supplementary Material Available: A listing of structure amplitudes, Tables III and V (12 pages). Ordering information is given on any current masthead page.

References and Notes

(1) (a) Department of Chemistry, Northwestern University. (b) Department of Electrical Engineering, Northwestern University. (c) Physics Division, Argonne National Laboratory.
(2) (a) Fellow of the Alfred P. Sloan Foundation. (b) Camille and Henry Dreyfus Teacher–Scholar.
(3) Cowie, M.; Gleizes, A.; Grynkewich, G. W.; Kalina, D. W.; McClure, M. S.; Scaringe, R. P.; Teitelbaum, R. C.; Ruby, S. L.; Ibers, J. A.; Kannewurf, C. R.; Marks, T. J. *J. Am. Chem. Soc.*, preceding paper in this issue.
(4) (a) Miller, J. S.; Epstein, A. J. *Prog. Inorg. Chem.* **1976**, *20*, 1–152. (b) Zeller, H. R. "Low-Dimensional Cooperative Phenomena", Keller, H. J., Ed.; Plenum Press: New York, 1975; pp 215–233.
(5) (a) Marks, T. J. *Ann. N.Y. Acad. Sci.* **1978**, *313*, 594–616. (b) Petersen, J. L.; Schramm, C. S.; Stojakovic, D. R.; Hoffman, B. M.; Marks, T. J. *J. Am. Chem. Soc.* **1977**, *99*, 286–288. (c) Marks, T. J.; Lin, L. -S., submitted for publication. (d) Marks, T. J.; Kundalkar, B., manuscript in preparation. (e) Schramm, C. A.; Stojakovic, D. R., Hoffman, B. M.; Marks, T. J. *Science* **1978**, *200*, 47–48. (f) Peterson, J. L.; Schramm, C. S.; Scaringe, R. P.; Stojakovic, D. R.; Hoffman, B.; Ibers, J. A.; Marks, T. J., manuscript in preparation.
(6) Burger, K.; Ruff, I. *Acta Chim. Acad. Sci. Hung.* **1966**, *49*, 1–19.
(7) Endres, H.; Keller, H. J.: Mégnamisi-Bélombé, M.; Moroni, W.; Nöthe, D. *Inorg. Nucl. Chem. Lett.* **1974**, *10*, 467–471.
(8) Endres, H.; Keller, H. J.; Moroni, W.; Weiss, J. *Acta. Crystallogr., Sect. B* **1975**, *31*, 2357–2358.
(9) Leichert, I.; Weiss, J. *Acta Crystallog., Sect. B* **1975**, *31*, 2877–2878.
(10) Leichert, I.; Weiss, J. *Acta Crystallogr., Sect. B* **1975**, *31*, 2709–2710.
(11) In ref 7, preliminary conductivity measurements were reported using silver paste electrical contacts. A time-dependent decrease in the conductivity was taken as evidence that the iodinated materials were reacting with the silver contacts.
(12) Marks, T. J.; Webster, D. F.; Ruby, S. L.; Schultz, S. *J. Chem. Soc., Chem. Commun.* **1976**, 444–445.
(13) Endres, H.; Keller, H. J.; Mégnamisi-Bélombé, M.; Moroni, W.; Pritzkow, H.; Weiss, J.; Comes, R. *Acta. Crystallogr., Sect. A* **1976**, *32*, 954–957.
(14) Brill, J. W.; Mégnamisi-Bélombé, M.; Novotny, M. *J. Chem. Phys.* **1978**, *68*, 585–592. NOTE ADDED IN PROOF. Structural data on monoclinic $Pd(bqd)_2$ have now appeared: Endres, H.; Mégnamisi-Bélombé, M.; Little, W. A.; Wolfe, C. R. *Acta. Crystallogr., Sect. B* **1979**, *35*, 169–171.
(15) Boyer, J. H.; Ellzey, S. E. *J. Am. Chem. Soc.* **1960**, *82*, 2525–2528.
(16) (a) Cornu, A.; Massot, R. "*Compilation of Mass Spectral Data*," Heyden and Son: London, 1968; p 28c. (b) Mass Spectral Data, American Petroleum Institute Research Project 144, 1948; p 251.
(17) See, for example, Waters, J. M.; Ibers, J. A. *Inorg. Chem.* **1977**, *16*, 3273–3277.
(18) See paragraph at end of paper regarding supplementary material.
(19) (a) Teitelbaum, R. C.; Ruby, S. L.; Marks, T. J. *J. Am. Chem. Soc.* **1978**, *100*, 3215–3277. (b) Kalina, D. W.; Stojakovic, D. R.; Teitelbaum, R. C.; Marks, T. J., manuscript in preparation.
(20) (a) Kiefer, W. *Appl. Spectrosc.* **1974**, *28*, 115–134. (b) Trotter, P. J.; White, P. A. *ibid.* **1978**, *32*, 323–324.
(21) (a) Herbstein, F. H.; Kapon, M. *Nature (London)* **1972**, *239*, 153–154. (b) Havinga, E. E.; Boswijk, K. H.; Wiebenga, E. H. *Acta. Crystallogr.* **1954**, *7*, 487–490. (c) Havinga, E. E.; Wiebenga, R. H. *ibid.* **1958**, *11*, 733–737.
(22) (a) Gibb, T. C. "Principles of Mössbauer Spectroscopy", Chapman and Hall: London, 1976; Chapter 4.2. (b) Bancroft, G. M.; Platt, R. H. *Adv. Inorg. Chem. Radiochem.* **1972**, *15*, 187–201.
(23) The staggering angle in the structures of $Ni(bqd)_2I_{0.018}$ and $Pd(bqd)_2I_{0.5}{\cdot}0.52\,o\text{-}C_6H_4Cl_2$ is the calculated dihedral angle between the M–N(1) bond of an $M(bqd)_2$ moiety and the M–N(2)′ bond of a nearest-neighbor $M(bqd)_2$ unit along the stacking axis.
(24) Robertson, J. M.; Woodward, I. *J. Chem. Soc.* **1937**, 219–230.
(25) Banks, C. V.; Barnum, D. W. *J. Am. Chem. Soc.* **1958**, *80*, 4767–4772.
(26) Williams, D. E.; Wohlauer, G.; Rundle, R. E. *J. Am. Chem. Soc.* **1959**, *91*, 755–756.
(27) Peng, S. -M.; Ibers, J. A.; Milar, M.; Holm, R. H. *J. Am. Chem. Soc.* **1976**, *98*, 8037–8041.
(28) Peng, S. -M.; Goedken, V. L. *J. Am. Chem. Soc.* **1976**, *98*, 8500–8510.
(29) Handbook of Chemistry and Physics", 57th ed.; Chemical Rubber Publishing Co.: Cleveland, Ohio, 1976–1977, p F-216.
(30) Endres, H.; Keller, H. J.; Lehmann, R.; Weiss, J. *Acta Crystallogr., Sect. B* **1976**, *32*, 627–628.
(31) (a) Miller, J. S.; Griffiths, C. H. *J. Am. Chem. Soc.* **1977**, *99*, 749–755. (b) Foust, A. S.; Soderberg, R. *ibid.* **1967**, *89*, 5507–5508. (c) Miller, J. S.; Goldberg, S. Z. *Inorg. Chem.* **1975**, *14*, 2294–2296.
(32) Calleri, M.; Ferraris, G.; Viterbo, D. *Inorg. Chim. Acta* **1967**, *1*, 297–302.
(33) (a) Hara, Y.; Shirotani, I.; Onodera, A. *Solid State Commun.* **1976**, *19*, 71–175. (b) Anex, B. G. ACS Symposium Series, No. 5, American Chemical Society: Washington, D.C., 1974; pp 276–300. (c) Ohashi, Y.; Hanazaki, I.; Nagakura, S. *Inorg. Chem.* **1970**, *9*, 2551–2556.
(34) (a) Stojakovic, D. R. Ph.D. Thesis, Northwestern University, Evanston, Ill., Aug 1977. (b) Gabes, W.; Stufkens, D. J. *Spectrochim. Acta, Part A* **1974**, *30*, 1835–1841. (c) Robin, M. B. *J. Chem. Phys.* **1964**, *40*, 3369–3377.
(35) Reddy, J. M.; Knox, K.; Robin, M. B. *J. Chem. Phys.* **1964**, *40*, 1082–1089.
(36) Without a Kramer–Kronig analysis of the reflectance data,[33b] the spectral maxima cannot be precisely related to the absorption maxima.
(37) (a) Phillips, T. E.; Hoffman, B. M. *J. Am. Chem. Soc.* **1977**, *99*, 7734–7736. (b) Phillips, T. E.; Scaringe, R. P.; Hoffman, B. M.; Ibers, J. A. Submitted for publication.
(38) (a) Shante, V. K. S. *Phys. Rev. B* **1977**, *16*, 2597–2612, and references cited therein. (b) Cohen, M. H. *Lect. Notes Phys.* **1977**, *65*, 225–262, and references cited therein. (c) Mihaly, G.; Ritvay-Emandity, K.; Janossy, A.; Holczer, K.; Grüner, G. *Solid State Commun.* **1977**, *21*, 721–724. (d) Mott, N. F. "Metal-Insulator Transitions," Taylor and Francis: London, 1974; Chapter 1.
(39) (a) Epstein, A. J.; Conwell, E. M.; Sandman, D. J.; Miller, J. S. *Solid State Commun.* **1977**, *23*, 335–358. (b) Epstein, A. J.; Conwell, E. M. *ibid.* **1977**, *24*, 627–630. (c) Conwell, E. M. *Phys, Rev. Lett.* **1977**, *39*, 777–780.
(40) Williams, J. M.; Petersen, J. L.; Gerdes, H. M.; Peterson, S. W. *Phys. Rev. Lett.* **1974**, *33*, 1079–1081.
(41) That is, the least-squares plane defined by the four coordinated nitrogen atoms.[27]
(42) (a) Whangbo, M.-H.; Hoffmann, R. *J. Am. Chem. Soc.* **1978**, *100*, 6093–6098. (b) Interrante, L. V.; Messmer, R. P. *Adv. Chem. Ser.* **1975**, *5*, 382–391. (c) Messmer, R. P.; Salahub, D. R. *Phys. Rev. Lett.* **1975**, *35*, 533–536.
(43) Miller, J. S. *Inorg. Chem.* **1977**, *16*, 957–960, and references cited therein.
(44) Cotton, F. A.; Wilkinson, G. "Advanced Inorganic Chemistry", 3rd ed.; Wiley-Interscience: New York, 1972; p 288.
(45) (a) Cowan, D.; Shu, P.; Hu, C.; Krug, W.; Carruthers, T.; Pochler, T.; Block, A. In "Chemistry and Physics of One-Dimensional Metals", Keller, H. J., Ed.; Plenum Press: New York, 1977, pp 25–47. (b) Herbstein, F. H. "Perspectives in Structural Chemistry", Vol. IV; Dunitz, J. D.; Ibers, J. A., Eds.; Wiley: New York, 1971; p 344. (c) Shchegolev, I. F. *Phys. Status Solidi A*, **1972**, *12*, 9–45.
(46) Williams, J.; Stang, P.; Schleyer, P. *Annu. Rev. Phys. Chem.* **1968**, *10*, 531–558.